

Article

# Underfloor Heating Using Ceramic Thermal Panels and Solar Thermal Panels in Public Buildings in the Mediterranean: Energy Savings and Healthy Indoor Environment

Víctor Echarri-Iribarren <sup>\*</sup>, Carlos Rizo-Maestre  and José Luis Sanjuan-Palermo

Department of Building Construction, University of Alicante, 03690 Alicante, Spain; carlosrm@ua.es (C.R.-M.); jls2@alu.ua.es (J.L.S.-P.)

<sup>\*</sup> Correspondence: Victor.Echarri@ua.es; Tel.: +34-965-903677

Received: 25 March 2019; Accepted: 13 May 2019; Published: 21 May 2019



**Featured Application:** Large format thermal ceramic panels (TCP), which work with water circulating through capillary tube mats, are excellent for construction applications. When applied to the floor for a radiant conditioning system, they provide excellent levels of comfort and save significant energy consumption.

**Abstract:** Radiant floor air conditioning systems based on capillary tube mats, in addition to offering high comfort standards, generate significant energy savings. They allow the use of renewable energies such as thermal solar panels and combine them with solar cooling systems based on lithium chloride or absorption systems with lithium bromide in summer, cooling water down to 15–16 °C through solar thermal panel energy collection. Thus, in addition to energy savings from the transport of low water flows, annual energy demand is also reduced. This research analyses the application of thermal ceramic panels (TCP)—containing polypropylene (PPR) tube capillary mats—to public buildings in the Spanish Mediterranean. A case study of the Museum of the University of Alicante (MUA) is presented. Water was distributed individually from a split system heat pump inside the building combined with a thermal solar panel system on the roof. The MUA’s annual energy demand was quantified using thermal simulation tools and was monitored during the entire one-year cycle. Simulations were conducted both for the radiant floor system and an all-air conventional convective system, as well as with solar thermal panel applications. The reduction in annual energy demand was 24.91% when TCP panels are used on the floor. This is a considerable value, but lower than others results obtained in Central Europe due to the higher values of humidity. When solar thermal panels are installed on the rooftop the energy savings can increase to 60.70%.

**Keywords:** thermal ceramic panel; capillary tube systems; solar thermal panels; energy saving; thermal comfort; renewable energy; solar refrigeration technology

## 1. Introduction

The 1980s saw the development of systems of conditioning of architectural spaces based on capillary mats of polypropylene tubes of about 3 mm in diameter, separated by approximately 10 mm. Cold or hot water circulates through these mats. They can be applied to any interior walls—floors, walls and ceilings—using a range of techniques—such as plasterboard, false ceilings, false walls or plaster projection, achieving healthy, silent and comfortable air conditioning. In addition, these radiant surface conditioning systems lead to notable energy savings compared to conventional air conditioning systems [1].

Radiant Surface Conditioning systems using PPR capillary mats work mainly by radiation, and secondarily by convection. When working by cooling or moderately heating some walls, with minimal dehumidification in summer, and without using cold or hot air impulsion, significant advantages are achieved with respect to convective systems. The sound level decreases dramatically, the air moves at very low convection speeds, which provides comfort, and summer air temperature is approximately 2 °C higher than in the case of convective systems. In this way, the comfort level increases significantly. In addition, notable energy savings are made, as certified by reputable research institutes. The main factors are the water's greater capacity to transport energy compared to that of air, the system's self-regulation, and the reduction of thermal loads as indoor air temperature is higher in summer [2].

Possible schematic diagrams of these capillary mat systems have been widely addressed in recent publications [3] (Figure 1). When working with water at moderate temperatures in both summer and winter, it is feasible to use alternative energies: solar panels, lithium chloride-based chemical energy accumulation systems [4,5], absorption systems, geothermal energy systems [6] or use of seawater [7], among others [8].

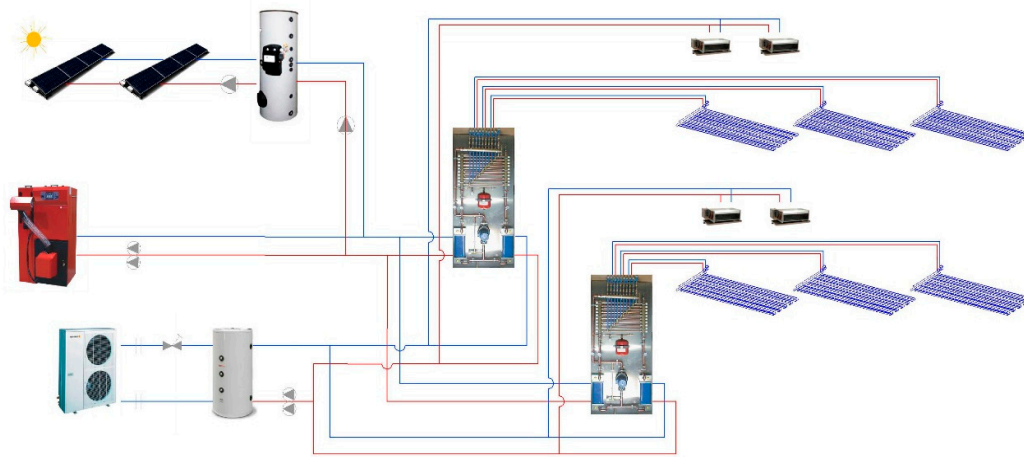


**Figure 1.** Schematic diagram of a capillary mat installation, with fan-coils for dehumidification, and control substations.

In recent years, ceramic materials have undergone huge technical improvements regarding mechanical resistance and behaviour towards external agents of humidity, temperature or UV radiation, presenting almost non-existent water absorption. To the inalterable nature of porcelain stoneware, we must add, as we will see later, the production of panels in large formats and thicknesses, enabling to use the material on ventilated facades, or interior linings in functional spaces other than bathrooms and kitchens.

In the present work, we studied the application of large-format thermal ceramic panels (TCP) to the floor of the Museum of the University of Alicante (MUA, by its Spanish acronym), with the aim of implementing radiant floor air conditioning. Previous studies presented the results obtained from applying TCP panels on walls and ceilings [9], instead of using plaster or steel sheets, but they did not apply them to floors. Novel 20 mm-thick large-format ceramic pieces allow us to apply the panels to flooring combined with the application of PPR capillary mats. It would be possible to condition the MUA in winter and summer, with a dehumidification system based on fan-coils, and obtain substantial energy savings. The option to incorporate a thermal solar panel system on the rooftop was also examined. In this way, in winter, a system of hot water production is applied, and water is cooled by chemical energy (solar cold), providing the system with alternative energy. As we will see, big energy savings were made, with acceptable amortisation periods regarding the installation's required investments.

## 2. Ceramic Thermal Conditioning Panel (TCP)

The research group of the University of Alicante “Technology and Sustainability in Architecture” developed and patented, together with ASCER and the ITC, a TCP panel of ceramic thermal conditioning in 2010 [10]. It consists of one or two pieces of large-format and low-thickness porcelain stoneware [11] reinforced with fiberglass on one of its faces, a capillary mat of polypropylene PPR tubes 3.5 mm in diameter separated every 10 mm, and conductive paste [12] to adhere it all together and embed the capillary mat (Figure 2). The initial dimensions were 300 cm × 100 cm × 3 mm, although larger panels of 320 cm × 160 cm × 9 mm are now being manufactured. The solution is ideal for modular ceramic ceilings, wall and ceiling-mounted large-format boards, or even for baffle type solutions, in which the panels are vertically suspended from the ceiling. When working with 3 mm, 3 + 3 mm or 9 mm pieces of prefabricated panels, one gains a great ease of on-site assembly, maintenance and replacement in case of leaks or malfunction.

These panels of porcelain stoneware and conductive paste are ideal to obtain suitable thermal conditioning. In fact, when equipped with thermal conductivity and high effusivity, the thermal capacity is similar to that of usual plaster panels. Though these parameters are four times lower in the case of metal roof sheets, the tests regarding the minimum running times to reach the project’s emission power, visualised via thermographs, were about ten minutes for plaster and stoneware low-thickness porcelain tiles, and five minutes for the metal roof. Some recent prototypes have been introduced in an office wall of the University of Alicante, in an all-water building, in which a management substation was installed, and the existing fan-coil connections were redirected towards distribution to four radiant panels measuring 2.5 × 1 m. (Figure 2). The conditions of comfort, time and emission power are currently satisfactory. These empirical data were applied to a Spanish Mediterranean home, with excellent results regarding comfort and energy consumption reduction [13].



**Figure 2.** Application of thermal ceramic panels (TCP) thermal ceramic panels in an office of the University of Alicante.

TCP ceramic panels also have other advantages over plaster finishes and metallic materials such as steel sheets. They are inert against chemical actions or processes of oxidation and degradation

through wear and tear. Mechanical resistance is greater as well: the wall application can be reinforced by adhering two ceramic pieces using a butyral, applying 3 + 3 mm. No maintenance is required, and replacement is simple. In the case of false ceilings, the low-thickness porcelain stoneware is light and does not suffer deformation or damage during maintenance operations. There are vast amounts of aesthetic possibilities, with an abundant choice of finishes, including the reproduction of images through the Inkjet technique [14,15] before the firing process.

### 3. Application of TCP Panels in the Museum of the University of Alicante

The Museum of the University of Alicante (MUA) is composed of a range of different volumes. Some rooms are semi-buried, and the rooftop is covered by a bed of water. The main room or “cube”, which is where we will apply the TCP panels, is an extensive, flexible space lined on the inside with bakelised wood boards, measuring  $63 \times 22.5 \times 9$  m (Figure 3). The configuration is based on passageways throughout its perimeter allowing circulation over three levels for maintenance tasks. The circulation under the roof also takes place through 8 passageways. This buffer space is used for all the building’s lighting, air-conditioning and water-evacuation installations (Figure 4). The roof includes 7 giant skylights with orientable aluminium external blades. The perimeter on the ground floor is made of simple glass, with MD panel-based protection.

The interior enclosure consists of white lacquered MD panels glued with polyurethane cord on timber frames, screwed on a steel tube substructure. The outer enclosure was made up of sandwich type panels with rock-wool insulation, phenolic outer panel, MD interior panel and timber frames on the periphery. The enclosure was damaged because of humidity, solar radiation and thermal differences caused by thermal bridges due to the insulation material’s discontinuity [16]. In 2010, the enclosure underwent an energetic rehabilitation. A total of 3 cm of projected polyurethane was applied to the existing skin, and a ventilated facade was generated, taking advantage of the existing metal substructure, with latest generation phenolic panels (Figure 5).



Figure 3. View of the Museum of the University of Alicante (MUA).

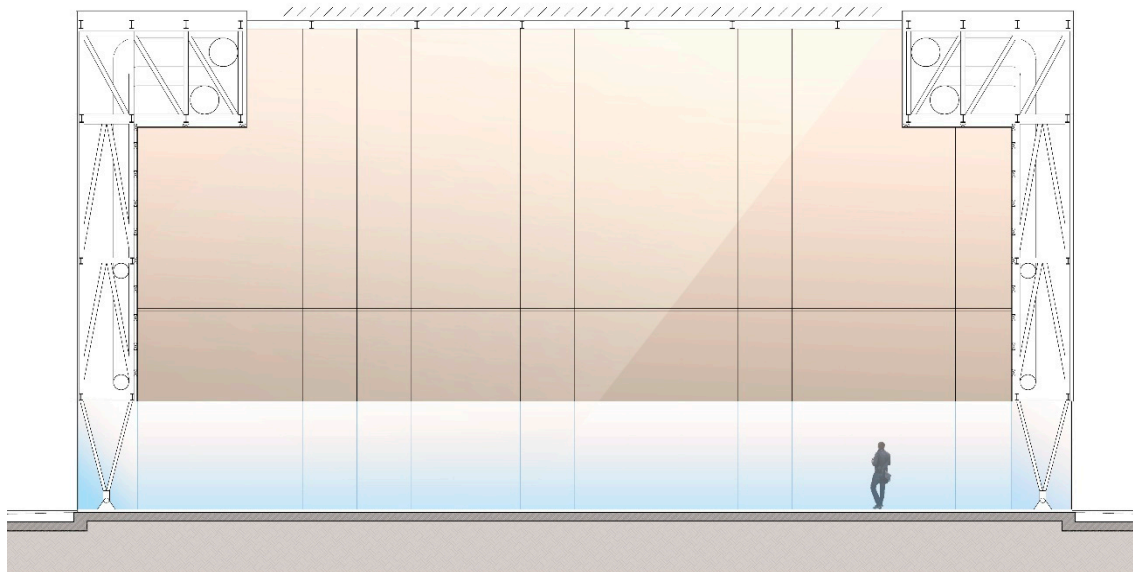


Figure 4. Cross section of the MUA, with passageway spaces in the enclosure.

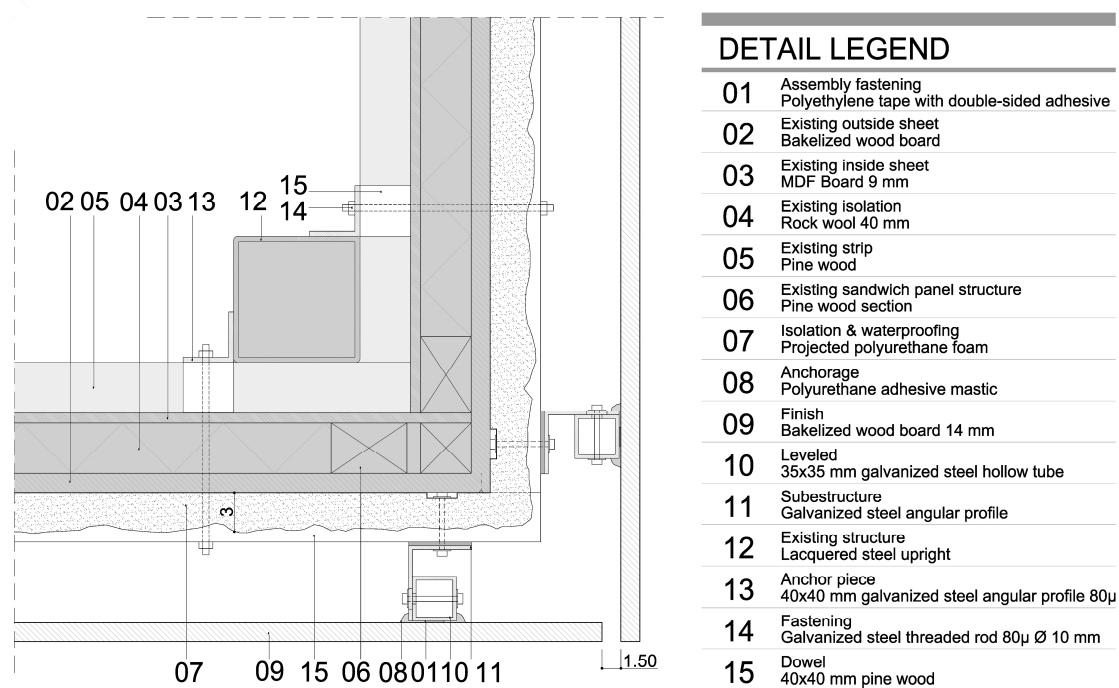
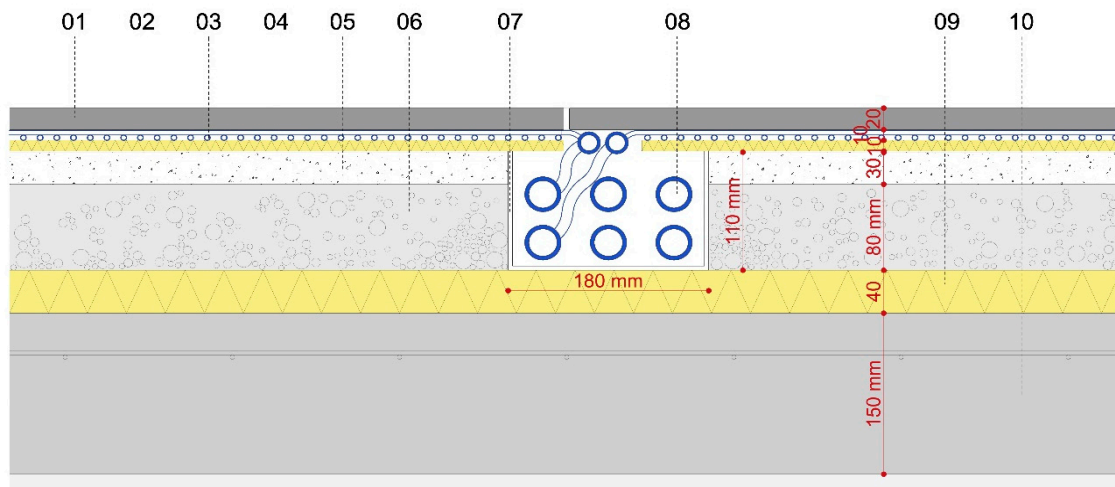


Figure 5. Constructive details of the MUA. Energy rehabilitation project.

The MUA's current air conditioning system is an all-air system, with a split heat pump system located inside the conduits in the top part, and primary air is distributed through fiberglass conduits. The air is renewed by means of rooftop inlets, in manholes with drains that avoid the inlets from protruding above the rooftop plane.

The present study was based on the hypothesis of replacing the MUA flooring with underfloor TCP panels. This would allow replacing the air conditioning system, which we will call Option 1 (OP1), by a radiant floor system based on hot water distribution in winter and cold water in summer, with a fan-coil dehumidification installation, hereon Option 2 (OP2). To do this, prefabricated panels would be used with pieces of latest generation 20 mm-thick porcelain stoneware (Figure 6). Hot or cold water

would be distributed using a 32 mm-outer diameter PPR pipe system, embedded in the flooring in 180 × 110 mm pipes. TCP panels, containing 3 mm PPR capillary tube mats, would be connected with flexible hoses and click and cool connections.



**Figure 6.** Ceramic thermal conditioning panel applied to the MUA floor. 01: Large-format porcelain stoneware piece. 300 × 100 × 2 cm. 02: Adhesive layer. Beka Thermal Conductive Paste V. WLP. 1. Thickness: 6 mm. 03: PPR capillary mat. Diameter: 3 mm. Separation: 10 mm. 04: Polyurethane foam thermal insulator. Thickness: 10 mm. 05: Regulatory layer. Self-levelling cement mortar. Average thickness: 10 mm. 06: Coating of screed: expanded clay. Thickness: 80 mm. 07: Aluminium channels to pass the PPR distribution pipes through. 08: PPR distribution pipes. Diameter: 32 mm. 09: Thermal insulator. Type IV expanded polystyrene. Thickness: 40 mm. 10: Reinforced concrete slab with electrowelded mesh 150 × 150 mm. Thickness: 150 mm.

### 3.1. Comparison of Operating Temperatures $T_o$

To compare the energy efficiency of both options, the user's comfort conditions must be similar. For this, we adjusted the similar operating temperature parameter  $T_o$ , and relative humidity RH in both scenarios.  $T_o$  is defined as "the uniform temperature of an imaginary enclosure in which a body exchanges the same dry heat (without taking into account latent loads) by radiation and convection than in an identical real environment". Once we determined experimentally and sufficiently closely, both the convection coefficients  $h_c$  according to the expression (1), and the radiation  $h_r$ —which adopts approximate values of 4.7 W/m<sup>2</sup>K at an estimated human body temperature  $T_i$  of 30 °C—we proceeded to calculate, for both established options, the operating comfort temperature  $T_o$ , values according to the expressions:

$$h_c = 14.11 \cdot v^{0.24} \text{ (W/K)} \quad (1)$$

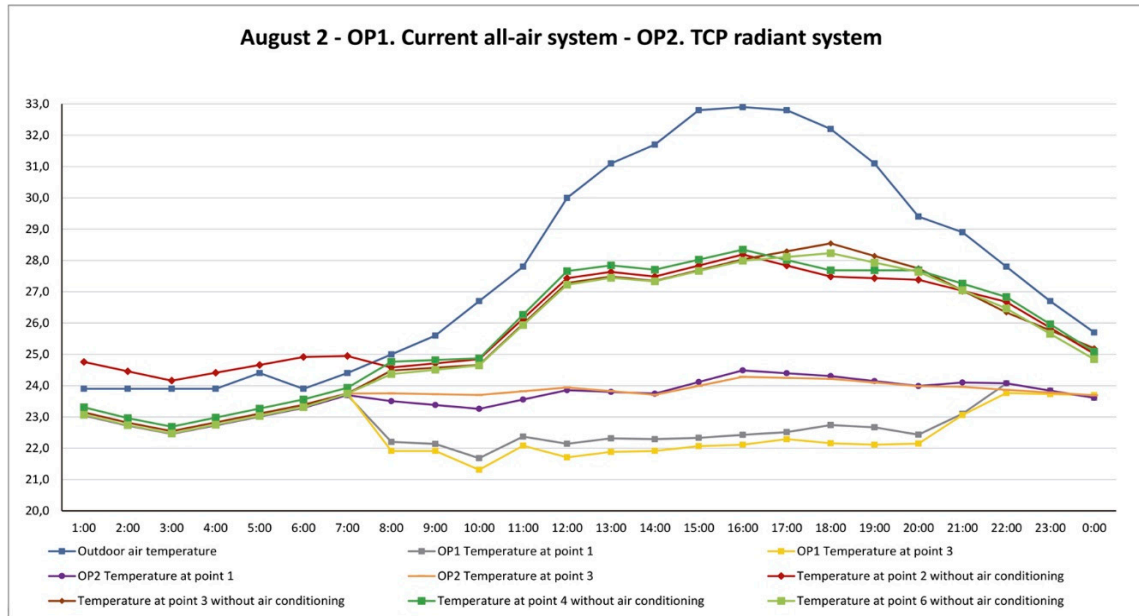
$$T_{mrt} = T_1 \cdot F_{P-1} + T_2 \cdot F_{P-2} + \dots + T_N \cdot F_{P-N} \quad (2)$$

$$T_o = \frac{h_r T_{mrt} + h_c T_a}{h_r + h_c} \quad (3)$$

The interpretation of this last expression (3) helps to understand how radiant surface conditioning systems work. An individual's feeling of comfort in closed spaces, with prior control of relative humidity and air velocity following Spanish Regulations on Heating Installations in Buildings (or RITE by its Spanish acronym) (between 40% and 60%, and 0.15 to 0.24 m/s respectively, according to the winter or summer regime), depends on the air temperature surrounding it and the surface temperature of the walls making up the space. As shown, in the case of the MUA, the indoor air temperature was about 2 °C higher in radiant systems compared to convective systems.

In Scheme 1, summer temperature values are observed for the 2 August 2015. They were obtained by monitoring the building, and by means of a Design Builder simulation for radiant systems with

TCP panel options. The outside air temperature values, the indoor air temperatures of the occupancy zone’s points 1 and 3 are shown for the current convective system (OP1) and the floor radiant panels system (OP2), and for indoor air temperature values in the event that the air conditioning system is not operating.



**Scheme 1.** Temperature of indoor and outdoor air in summer, with an all-air system, underfloor TCP ceramic panels, and no air conditioning. OP1: Option 1; OP2: Option 2.

As can be seen in Table 1, the operating temperatures  $T_o$  get close to the values of 23 °C introduced in the Design Builder simulations for the summer regime, as required by the RITE. By providing a large surface focal spot on the floor, ceiling or wall, the surface temperatures of the heat or cold-emitting focal spot become more moderate in these systems. The same emission power is achieved in the other systems and with similar operating temperature. As we will see, this difference generates substantial energy savings, and allows using alternative energies, such as solar [17,18], aerothermal or geothermal [19,20].

**Table 1.** Calculation of indoor air temperature  $T_a$ , mean radiant temperature  $T_{mrt}$ , and operating temperatures  $T_o$  in summer for both options.

	$v$	$h_c$	$T_a$	$h_r$	$T_{mrt}$	$T_o$
		$h_c = 14.11v^{0.24}$				
	m/s	W/K	K	W/m <sup>2</sup> K	K	K
OP1	0.068	7.402	22.11	4.70	24.45	23.02
OP2	0.036	6.354	25.63	4.70	20.05	23.26

### 3.2. Prior Considerations of Underfloor TCP Panels Usage

To conclude this comparative analysis of the installation of radiant floor TCP panels, we can say that comfort in the winter regime would be optimal, with an adequate temperature gradient in the living area, and, as we will see, a significant energy consumption reduction. When operating with air temperatures around 2 °C below that of convective systems, the air does not notably dry up and a humidification system is not required. In summer, the system would produce a satisfactory temperature gradient, cooling the indoor air in occupancy areas, as well as the glazed walls. Indoor air temperature  $T_i$  would be 2–3 °C higher than that produced in all-air convective systems. This

significantly reduces the thermal loads resulting from heat flows through the enclosures. The biggest downside of placing TCP panels on a ceiling or wall would be the risk of floor surface condensation, which would make the space impracticable. The indoor air should be dehumidified with a fan-coils system located in the conduits and limiting the water distribution temperature in the capillary mats by means of condensation control [12,21].

#### 4. MUA Monitoring

As indicated above, the MUA was monitored during the complete cycle of the year 2014, with more than 30 sensors of surface temperature, indoor and outdoor air temperature, relative humidity, pyranometer, indoor air velocity, etc. The monitoring system was designed to be wireless. The surface temperature sensors are connected to small analysers, model “EL-WiFi-TC-Thermocouple Probe Data logger”. Other types of “EL-Wifi-TH Temperature and Humidity Data Logger” analysers, with built-in indoor air temperature and relative humidity sensors, interpret the recorded data [22] and send wifi signals to a “RouterOS” model router. That router is connected to a laptop computer (Figure 7). By installing the “EasyLog Wifisoftware”, the data sent by the analysers is received and stored on the computer. The data is sent daily to a virtual disk and using a personal code, the information can be accessed from any network point. In addition, a small station was installed on the roof of the building with sensors of outside air temperature, relative humidity and a pyranometer (Kipp Model CMP3 Pyranometer Iso Second Class) to measure solar radiation.



**Figure 7.** Wireless monitoring system. Reception of the router and data processing laptop.

To adjust the simulation parameters to the actual data, or to calibrate the model, we used the climate file obtained on site and validated using the climatological data recorded by the weather station of the climatological Laboratory of the University of Alicante. We also modified the value of air infiltration through the enclosures, using the Design Builder simulation tool, to adjust the annual energy demand obtained according to real energy consumptions provided by the Vice-Rectorate of the Campus and Technology of the University of Alicante. Average energy consumption over the 2010–2014 period

was 203,050 kWh/year. Once the lighting consumption value was discounted—2.8 kWh/m<sup>2</sup>y—the value of 197.5 MWh/y was obtained for the existing all-air conditioning system. The same methodology was followed to adjust indoor surface temperatures and indoor air temperature. Fixing the set temperature at 21 °C in winter and 24 °C in summer facilitated the calibration process, in addition to the fact that users cannot adjust the standards of air conditioning in a personalised way. The activation time of the all-air installation was from 9 a.m. to 8 p.m.

The scale and constructive conditions of the MUA's access doors prevented us from performing The Blower Door test in the MUA. To obtain the mean calculation value of the building's air infiltration—a difficult parameter to quantify—and to be able to perform the simulations in Design Builder, we resorted to results obtained in recent research, with test measurements of similarly constructed buildings around Alicante [23]. Simulations were also performed using Design Builder to adjust or calibrate the model according to the energy consumption obtained from the installation's electrical meter measurements. We proceeded to perform simulations with an all-air impulsion system, and determined that the actual renewal air volume value was 2 air changes per hour (acH). Once these prior values were obtained, the protocol established by the UNE-EN-ISO 13790:2011 standard [24] was followed, applying the value obtained from the 50 Pa ( $n_{50}$ ) pressure test. The result was 0.842 acH, a high value for a building of this nature, with a low form factor value. This high infiltration value is due to the building's construction characteristics. The joints between phenolic panels had been filled with silicone, which had been deteriorating over the years. The same applied to the silicone joints of the Stadip simple glass on the ground floor. The rooftop had the same problem, as it had been executed dry, with deficient joints between the sandwich panels and the skylights.

The Thermographic camera ThermaCam P 25 of Flyr was used to detect thermal bridges [25], and their effects were substantially mitigated after the enclosure's rehabilitation. The continuous projection of polyurethane foam reduced the thermal transmittance  $U$  values and linear thermal transmittance  $\Psi$  in joints and structural points [26,27]. Quantification was performed using the AnTherm software: load gains or losses due to thermal bridges were estimated at 3.5% of total thermal loads [28] due to thermal transmittance  $U$  of the enclosures, a value that was similar to that obtained in previous studies [29,30].

## 5. Calculating the MUA's Energy Demand

Spanish regulations on energy efficiency in buildings make it compulsory to fill out the technical document DB-HE on energy saving [31,32], which is part of the Technical Building Code (or CTE by its Spanish acronym). The regulation requires you to apply the standardised tool Lider-Calener (HULC) [33] to architectural projects. The tool models the project and applies a climate file, incorporated in the tool, depending on the location and altitude of the building site. You can obtain the annual energy demand value by simulation, and the energy rating according to the air conditioning systems and energy sources used in the building. This tool is a breakthrough for energy efficiency improvement. Nevertheless, it is still far from providing a simulation adjusted or calibrated according to buildings' actual behaviours. It also presents some shortcomings. For example, it does not allow to introduce bioclimatic techniques, or take into account the fact that certain energies are used predominantly over others, due to energy policies that are often not sufficiently justified [34]. Compared to HULC, other simulation tools such as Design Builder or TRNSYS allow adjusting to actual building use, such as opening or closing windows according to time slots or using the enclosures' thermal inertia for thermal comfort and reducing energy demand through phase change materials [35]. The Design Builder tool has been used for this research. Its reliability through the use of the EnergyPlus calculation engine has been extensively tested.

To perform the MUA's behaviour simulations in terms of annual energy demand and control of interior comfort parameters, the building was modelled (Figure 8), and the following data was introduced into the Design Builder tool:

1. The winter period covers 1 December to 30 April, and summer covers 1 May to 30 November. These are the usual weather conditions of San Vicente del Raspeig (Alicante) where the University of Alicante is located.
2. The temperature of indoor air is 21 °C in winter and 24 °C in summer. Relative humidity (RH) remains at 50%.
3. Occupancy, for the standard calculation of air renewal, is 709 people, 0.5 people per m<sup>2</sup>. According to current Spanish Technical Building Code (CTE) regulations, a value of 2.5 acH is required for air renewal, with 12.5 l/s per person. This high value was adjusted to the model calibration in Design Builder, with an average real occupancy of 100 people during visitor peak times, resulting in an air renewal of 0.36 acH. The energy demand was thus adjusted to the MUA's actual energy consumption.
4. Air infiltration through the enclosure was high, although it was moderated thanks to the application of continuous polyurethane foam during the MUA rehabilitation in 2010. As indicated, the quantification was performed thanks to a comparison with the Blower Door test carried out in similarly constructed buildings around Alicante [23]. The test was conducted in accordance with European Regulation EN 13829, using BlowerDoor GmbH MessSysteme Für Luftdichtheit equipment (Figure 7). The adopted value was 0.864 acH.
5. We estimated load gains or losses due to thermal bridges at 3.5% of total thermal loads [28] by thermal transmittance  $U$  of the enclosures [27,36], which were obtained on site by means of the multifunction instrument KIMO TM210 by Testo [37]. A ThermaCam P25 thermographic camera was used for detection and quantification.

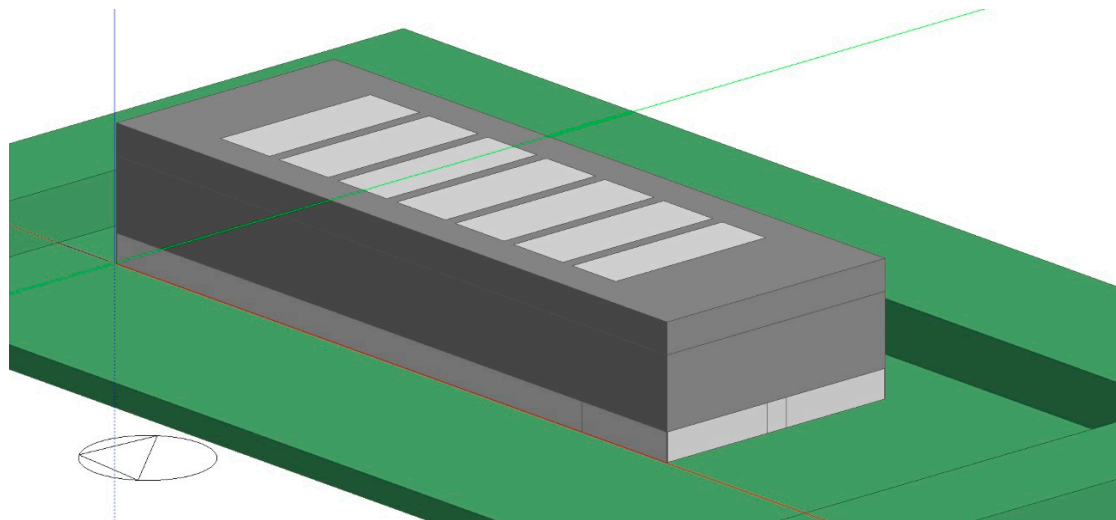


**Figure 8.** Model of the MUA in Design Builder.

The schematic diagram of the capillary tube mats project was introduced into the Design Builder model (Figure 9). Several strategies were adopted to adjust the parameters obtained by simulation to the actual data, to calibrate the model. First, energy consumption data were obtained from electrical meters in the building. The surface temperatures of the TCP panels were then pre-set to 17 °C, to avoid surface condensation. We also introduced the climate file relating to external air temperatures, relative humidity and solar radiation levels by pyranometer throughout a complete one-year cycle, obtained for Alicante in previous works [9]. Lastly, the walls' surface temperature was corrected, and the infiltration value was adjusted to 0.342 acH, so the model was calibrated by adjusting the temperatures of the air and walls to the monitoring values [22]. We also applied the dehumidification of the ten fan-coils, with a total power of 25 kW and an energy consumption of 27,854 kWh/y.

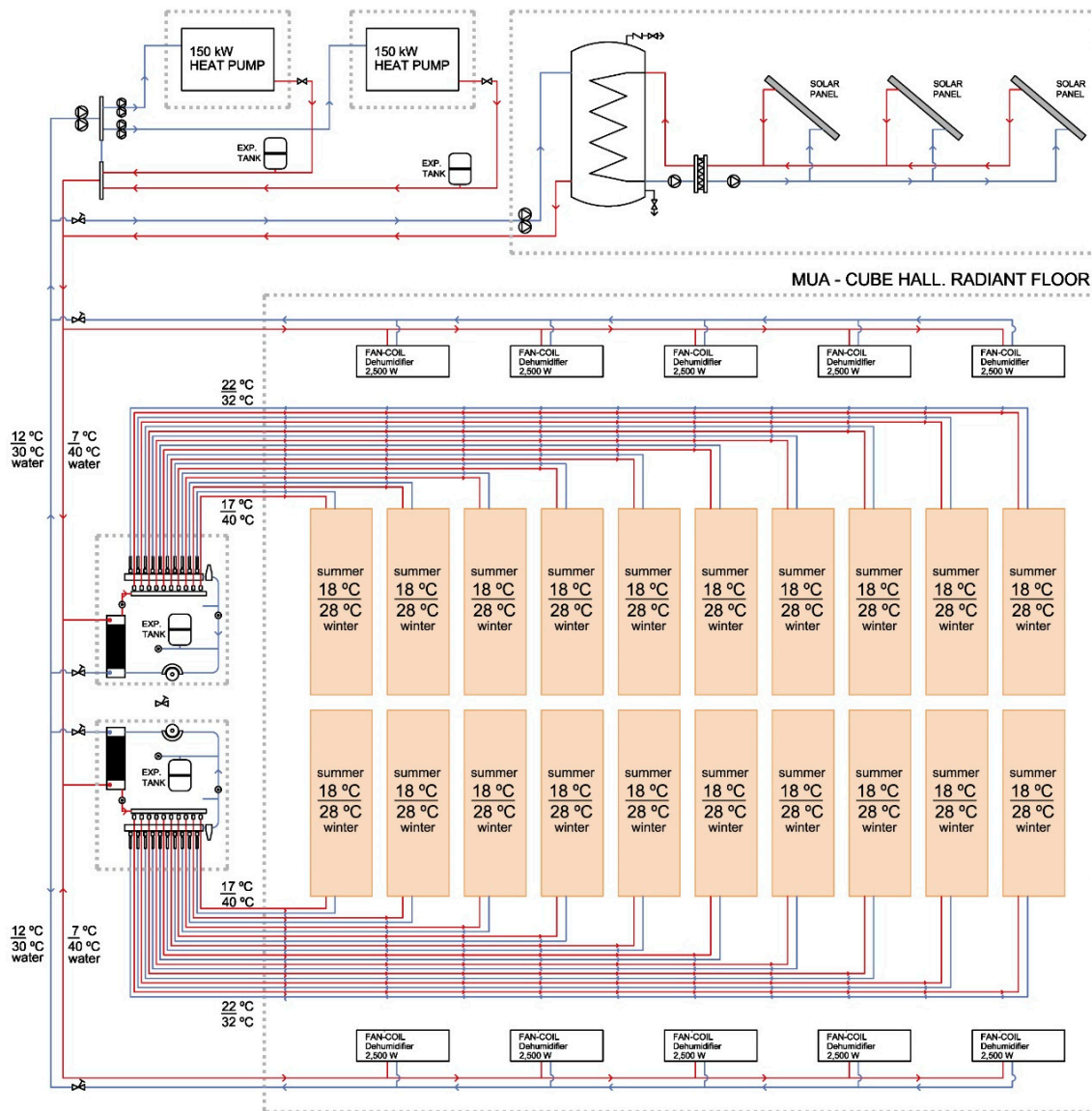


**Figure 9.** Schematic diagram of the installation of capillary mats and fan-coil dehumidification modelled in Design Builder.

### 5.1. Annual Energy Demand with TCP Panels and Comfort Conditions

Once the air renewal rate parameters above were obtained according to the CTE—air infiltration, surface temperatures, occupancy, etc.—and we had calibrated the model, we simulated the MUA’s behaviour according to the two options described above. The possibility of incorporating solar thermal panels on the rooftop combined with TCP panels has been studied:

OP1. All-air installation based on reversible air-air heat pump split system, model XPOWER VRF 2 Tubes (38VT-168HTEE) and air conditioner 39SQ flow rate 1.8 m<sup>3</sup>/s by Carrier, with 148 kW cooling power and 162 kW heat power. Condenser and climate control in the MUA’s conduit, with cold or hot air distribution throughout the building’s whole volume.

OP2. Installation of PPR capillary tube mats, in TCP panels, with an air-water heat pump model Aquasnap 30RQSY039-160 by Carrier, 148 kW cooling power and 162 kW heat power similar to OP1, distribution of water to two distribution substations located in the MUA’s conduits, and water distribution in the secondary circuit by a total of 24 independent PPR 32 mm in diameter circuits per

floor, and ten fan-coils strategically located for air dehumidification, each with a cooling power of 2.5 kW.

OP3. Installation of PPR capillary tube mats similar to that of OP2, with the same heat pump as above, and the ten fan-coils for air dehumidification, with a system of 230 m<sup>2</sup> of solar thermal panels, with absorption cooling, chemical energy (solar cooling). They provide alternative energy to the system.

Table 2 shows the results of thermal loads, solar gains by glazing and internal thermal loads for OP1 and OP2. They can be observed to be very high, boosted by the presence of giant rooftop skylights lacking protection, despite having been later covered with sandwich panels. As can be seen, using TCP panel radiant systems would reduce these thermal loads by 18% in the case of the OP2 radiant floor, and by 17.2% in the case of the radiant wall. The most decisive factor, apart from the energy provided by the equipment located inside the MUA, was the indoor air temperature  $T_i$ , increase in summer and decrease in winter, with similar comfort levels to that of convective systems, which produces a substantial decrease in heat flows by  $U$  transmittance on all exterior walls.

**Table 2.** Calculation of energy demands. Current state, radiant floor OP2 and radiating walls OP3.

	OP1 MUA 2000		OP2 TCP Radiant Floor	
	Summer	Winter	Summer	Winter
	Wh/m <sup>2</sup> y	Wh/m <sup>2</sup> y	Wh/m <sup>2</sup> y	Wh/m <sup>2</sup> y
Enclosure				
Glazing	15,733	20,069	8716	18,341
Walls	1689	216	814	251
Floors-ground	−1506	6367	−1403	5002
Partitions	0	0	0	0
Rooftops	5279	7115	2452	4835
Outdoor floors	310	167	296	138
Infiltration	12,193	21,532	6393	17,031
	<b>36,119</b>	<b>54,211</b>	<b>17,268</b>	<b>45,599</b>
Loads				
Lighting	2414	2833	2414	2833
Equipment	3766	2658	1219	1050
Occupation	8956	6975	8956	6975
Solar gains	38,541	−25,637	38,541	−25,637
	<b>53,671</b>	<b>−13,171</b>	<b>51,177</b>	<b>−14,779</b>
	kWh/m <sup>2</sup> y	kWh/m <sup>2</sup> y	kWh/m <sup>2</sup> y	kWh/m <sup>2</sup> y
Primary energy	<b>89.79</b>	<b>41.04</b>	<b>67.43</b>	<b>30.82</b>

Table 3 shows the results by simulating summer, winter and annual energy demands for the three options OP1–OP3. These values are similar to those usually experienced in office buildings, in which 30% and 35% energy savings compared to convective systems were accredited in Central Europe [38]. In our case study, the simulations produced notable annual energy saving values. Annual energy demand was 130.83 kWh/m<sup>2</sup>y for the all-air system currently adopted, and 98.25 kWh/m<sup>2</sup>y for the TCP ceramic thermal panels underfloor system (OP2), accounting for 24.91% in energy savings. These reductions are of the same order of magnitude as those obtained in other studies [21,38]. In the case of radiant wall or ceiling systems, energy demand reductions were somewhat lower [1]. Figures 10 and 11 show the temperature gradients produced in the simulation in different areas of the house for both the OP1 and OP2 conditioning system options, which show homogeneous temperatures in the occupancy area for Radiant Systems. In addition, the indoor air temperature  $T_i$  was about 3 °C higher in summer and 2 °C lower in winter.

**Table 3.** Calculation of energy demands and CO<sub>2</sub> emissions of the 3 OP.

	OP1	OP2	OP3
Energy demand in summer kWh/m <sup>2</sup>	89.79	67.43	35.91
Energy demand in winter kWh/m <sup>2</sup>	41.04	30.82	15.39
Annual energy demand kWh/m <sup>2</sup> y	130.83	98.25	51.30
Annual CO <sub>2</sub> emissions in use stage	50,071.91	37,603.22	19,633.17
<b>Percentage</b>	<b>100.00%</b>	<b>75.09%</b>	<b>39.21%</b>

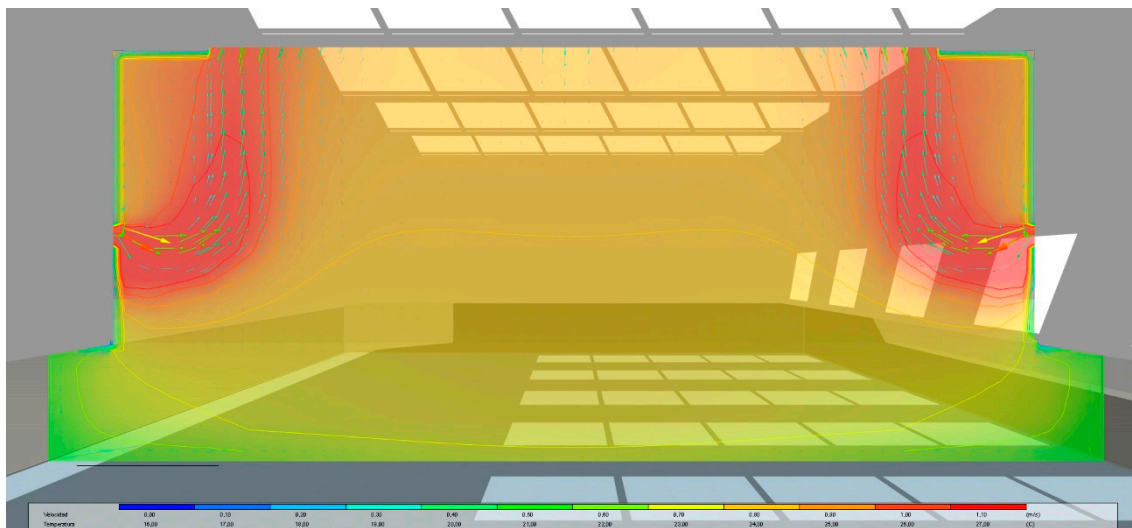


**Figure 10.** Computational fluid dynamics (CFD) graphic of the existent all-air system. Cross section of the MUA. Indoor air temperatures. 1 February 2015. 9:00 a.m.

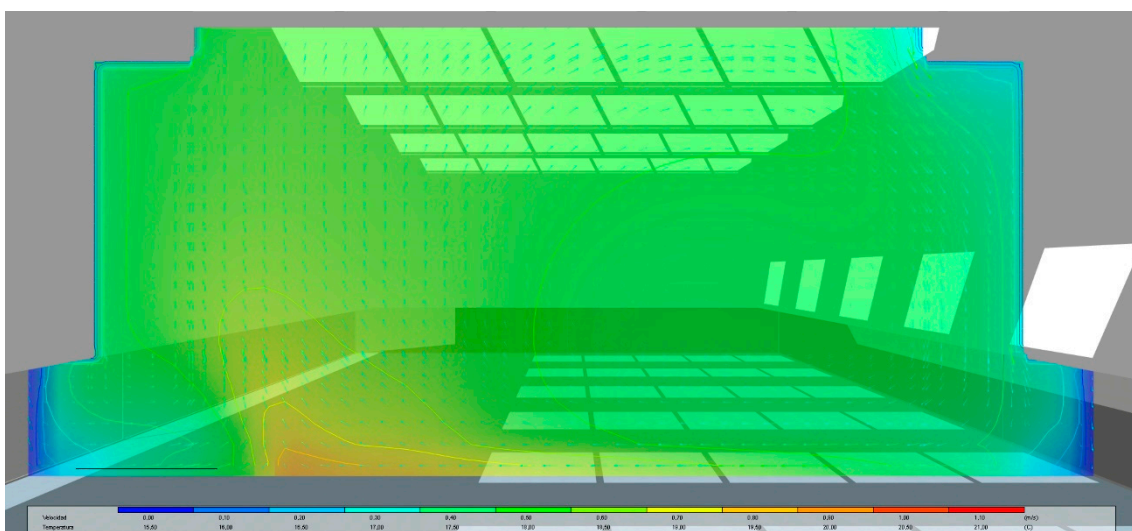
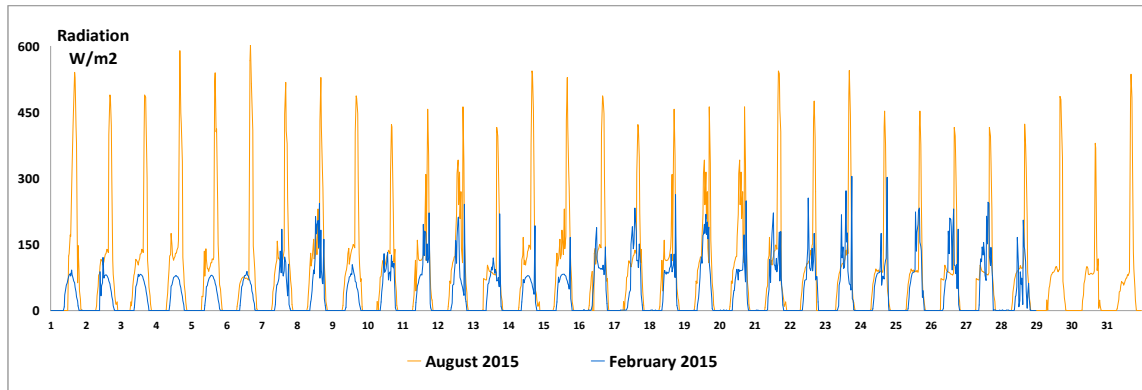


**Figure 11.** CFD graphic of the applied radiant floor system based on TCP panels. Cross section of the MUA. Indoor air temperatures. 1 February 2015. 9:00 a.m.

*5.2. Incorporation of Thermal Solar Panels to the TCP Panel Installation*

The energy savings gained by incorporating a system of thermal solar panels on the rooftop into the installation of air conditioning based on radiant floor TCP panels (OP3) will be analysed [39]. These solar thermal panels operate by heating the system’s water in winter or cooling it in summer by means of an absorption cooling system [40,41], or chemical energy (solar cold) [42,43]. The solar radiation power data on the MUA’s rooftop were collected during the complete year 2015 cycle, by

means of the pyranometer installed on the wireless monitoring system described above. Scheme 2 shows the radiation values obtained for the months of August and February. Table 4 shows the daily average values of energy collected each month, as well as total days of sunshine. These values were compared with other sources and recent publications that collected these values for the Spanish Levante; correlated values were obtained [42,44].



**Scheme 2.** Solar radiation Values captured on site for the months of August and February 2015.

The installation dimensioning was performed according to the load calculations using Design Builder (Table 2), after calibrating the model using the surface temperatures and indoor air temperature monitoring results. An installation of 230 m<sup>2</sup> of thermal solar panels is required for a yearly air conditioning energy demand of 98.25 kWh/m<sup>2</sup>y with an installation of two 150 kW power heat pumps in cold mode in summer. Based on the usual performance of these facilities based on the sun, these panels contributed 62.2% to the system during energy demand peaks in summer in the case of maximum sunshine [20]. The installation performance of 230 m<sup>2</sup> of solar thermal panels, with a 38° latitude and a 45° inclination, was 71.4% [45]. Taking into account that overall installation performance was 84.5% [46], total energy contribution to the TCP panel radiant floor system, using water in winter, and a solar cooling system with energy storage by lithium chloride (LiCl) was 66,559 kWh/y.

**Table 4.** Solar energy received per days, months and year.

Month	No of Days	Direct Irradiance (kWh/m <sup>2</sup> year)	Diffuse Irradiance (kWh/m <sup>2</sup> year)	Direct Energy per Month (kWh/m <sup>2</sup> )	Diffuse Energy per Month (kWh/m <sup>2</sup> )	Total Energy per Month (kWh/m <sup>2</sup> )
January	31	1.66	0.95	51.46	29.45	80.91
February	28	2.31	1.18	64.68	33.04	97.72
March	31	3.03	1.67	93.93	51.77	145.7
April	30	4.30	1.83	129	54.9	183.9
May	31	4.65	2.26	144.15	70.06	214.21
June	30	5.40	2.25	162	67.5	229.5
July	31	5.56	2.17	172.36	67.27	239.63
August	31	4.65	2.17	144.15	67.27	211.42
September	30	3.79	1.66	113.7	49.8	163.5
October	31	2.69	1.30	83.39	40.3	123.69
November	30	1.84	0.97	55.2	29.1	84.3
December	31	1.44	0.83	44.64	25.73	70.37
<b>Annual radiation</b>				<b>1258.66</b>	<b>586.19</b>	<b>1844.85</b>

The results obtained by the Design Builder simulation were calibrated and corrected using these on-site solar energy results [13] and compared to other studies on thermal energy in similar climates [42,47,48]. The system’s energy savings were of 60.79% compared to all-air convective systems

(Table 3). These are substantial values and they reflect the viability of these radiant TCP panel systems with rooftop thermal solar panels.

As illustrated, the energy consumption of the all-air system with split heat pump machines to distribute air in OP1 is 133% higher than that of the installation of water distribution to TCP panels in OP2 and OP3. Furthermore, it is 255% higher than that of OP3 with solar thermal panels. The energy consumption of OP2 is 24.91% less than that of OP1 or the all-air system, for the reasons described in paragraph 1. Consumption due to dehumidification, with the two fan-coils of OP2 and OP3 is 39.36 MWh/y, i.e., 30.08% of the total consumption of OP1, which would mean the installation of TCP panels would be a priori more unfavourable. However, the savings derived from the energy needed to transport the water compared to that of the air, as well as the thermal load reductions by reducing the thermal gap of the heat flow through the enclosures, means the system leads to substantial energy savings compared to OP1 overall.

CO<sub>2</sub> emissions were also quantified in the electrical mix to obtain an initial estimate of environmental impacts, based on the ELCD database [49]. According to this estimate, to produce 1 electric kWh, a total of 0.41 kg CO<sub>2</sub>, 0.00122 kg CH<sub>4</sub> and 0.0000465 kg N<sub>2</sub>O are released. Once final energy consumption from the user perspective was quantified for all the options OP1 to OP3, yearly CO<sub>2</sub> emissions could be quantified during the user stage. To finish, the system's primary energy consumption and CO<sub>2</sub> emissions were calculated using the factors of the Institute for Diversification and Saving of Energy (IDAE by its Spanish acronym) for 2010 [50], specifically: 2.21 MWhp/MWhf and 0.27 tCO<sub>2</sub>eq/MWh (Table 3).

## 6. Conclusions

Radiant surface conditioning systems based on PPR capillary tube mats provide high standards of comfort and significant energy savings over convective air delivery systems. Large-format thermal ceramic panels TCP have been applied to the floor of the University Museum of Alicante (Spain), containing capillary tube mats. Three scenarios were studied. The first scenario was based on an existing air conditioning system by means of all-air conditioning and duct distribution (OP1). In the second, a radiant surface heating system, based on radiant floor TCP ceramic thermal panels with embedded PPR capillary mats was applied (OP2). The third scenario was a variant of the latter one: it incorporated a system of solar thermal panels on the rooftop providing renewable energy to the system (OP3). The following results were obtained:

- The TCP panels system, thanks to the porcelain stoneware's high thermal conductivity and the capillary mats embedded in the panels, were shown to be more efficient energy-wise, and more comfortable than OP1. Annual energy demand was 24.91% lower in OP2 than OP1.
- If 230 m<sup>2</sup> of solar thermal panels were also installed on the rooftop with water storage tanks, for a triple phase absorption system by chemical energy accumulation using lithium chloride (LiCl), the energy savings would be considerable: 60.79% saved compared to OP1 and 47.79% compared to OP2.

The reduction in annual energy demand (24.91%) was around 20–30% below that obtained in other buildings on Spain's Mediterranean coast: 31.85% in a stand-alone single-family house, and 36.35% in offices of the University of Alicante. These differences are due to the installation's distinct scale: a more demanding regime of use is required in terms of  $T_i$  and RH conditions. The application of thermal solar panels on the rooftop, used as an active solar system in contrast to passive conditioning systems, was shown to be more efficient, both in heating and cooling modes by means of the chemical energy system (LiCl). When associated with TCP panels, the reduction of annual energy demand could reach 47.79%, compared to 20.25% obtained in the case of facade greenhouses, or 38.85% in the case of using the basement as a passive cooling system in summer and indoor air temperature moderation  $T_i$  in winter.

In future studies, we will analyse the feasibility of implementing radiant surface conditioning systems in public cultural buildings. Required return on investment and amortisation periods will be calculated, while energy cost reductions will be quantified as well as surcharges due to the installation of TCP panels with capillary mat water distribution and substation management.

**Author Contributions:** Conceptualisation, methodology, TCP panels design and application, funding acquisition, V.E.-I.; investigation, writing—original draft preparation, V.E.-I.; control of the data collecting of the monitorisation system and graphics, C.R.-M.; simulations by Design Builder, J.L.S.-P.; calibration of the model in Design Builder, and interpretation of data results, V.E.-I.

**Funding:** This research has been funded by the projects “Generation of knowledge on the multisensory interaction of human beings with the environments for the development of new products and services in the ceramics sector (4SENSES)” (ACOMP/2010/040). Complementary aid for R+D+i projects. Generalitat Valenciana. Ministry of Education. Spain, 2010; and “Research on sustainable architectural and bioclimatic conditioning solutions using ceramic materials (ASCER1-17I)”. Spanish Association of Manufacturers of Ceramic Tiles and Flooring (ASCER). 2015–2017.

**Acknowledgments:** Our thanks to Ginés Gómez Castelló, for his helping in the monitorization of the MUA, and TCP panels mounting; and to Francisco José Aldea and Justo Romero for their help with the Blower-Door test measurements.

**Conflicts of Interest:** The funders had no role in the design of the study; in the collection, analyses, or interpretation of data; in the writing of the manuscript, or in the decision to publish the results.

## References

1. Stetiu, C. Lawrence Berkeley National Laboratory. Energy and peak power savings potential of radiant cooling systems in US commercial buildings. *Energy Build.* **1992**, *30*, 127–138. [CrossRef]
2. Manual de Climatización Tranquila. Available online: <http://www.movinord.com/descargas/Climatizacion%202008.pdf>. (accessed on 11 March 2019).
3. Echarri, V.; Sánchez, R. Climatización por Superficies Radiantes Mediante Tramas Capilares. In *Arquitectura Eco-Eficiente*; Hernández Minguillón, R., Irulegi Garmendia, O., Aranjuelo Fernández-Miranda, M., Eds.; Servicio Editorial de la Universidad del País Vasco: San Sebastián, Spain, 2019; Volume II. (In press)
4. Climate Well™ 10. *Design Guidelines*. Available online: [http://www.solarcombiplus.eu/docs/SolarCombi\\_ClimateWell\\_trainingmaterial5.pdf](http://www.solarcombiplus.eu/docs/SolarCombi_ClimateWell_trainingmaterial5.pdf) (accessed on 12 July 2017).
5. Monné, C.; Alonso, S.; Palacín, F. Evaluación de una instalación de refrigeración por absorción con energía solar. *Inf. Tecnol.* **2011**, *22*, 39–41. [CrossRef]
6. Zamora, M. Empleo de bombas de calor acopladas a intercambiadores geotérmicos: Proyecto Geocool. *Montajes Instal. Rev. Técnica Sobre Constr. Ing. Instal.* **2008**, *38*, 66–72.
7. Haiwen, S.; Lin, D.; Xiangli, L. Quasi-dynamic energy-saving judgment of electric-driven seawater source heat pump district heating system over boiler house district heating system. *Energy Build.* **2010**, *42*, 2424–2430. [CrossRef]
8. Li, Z.; Songtao, H. Research on the heat pump system using seawater as heat source or sink. *Build. Energy Environ.* **2006**, *25*, 34–38.
9. Echarri Iribarren, V.; Galiano Garrigós, A.L.; González Avilés, A.B. Ceramics and healthy heating and cooling systems: Thermal ceramic panels in buildings. Conditions of comfort and energy demand versus convective systems. *Inf. Constr.* **2016**, *68*, 19–32.
10. Panel de Acondicionamiento Térmico Cerámico. Víctor Echarri (UA), Elena Oviedo (ASCER) y Vicente Lázaro (ITC), Patente de nº solicitud P201001626. INVENES. OEPM—Oficina Española de Patentes y Marcas. Available online: <http://invenes.oepm.es/InvenesWeb/detalle?referencia=P201001626> (accessed on 10 March 2019).
11. Zanelli, C.; Raimondo, M.; Guarini, G.; Marani, F.; Fossa, L.; Dondi, M. Porcelain Stoneware large Slabs Processing and Technological Properties. In Proceedings of the XI Congreso Mundial de la Calidad del Azulejo y del Pavimento QUALICER 10, Castellón, Spain, 15 February 2010.
12. Beka. *Technical Information G0*; Beka Heiz-undKülmatten: Berlin, Germany, 2000.
13. Echarri-Iribarren, V.; Rizo-Maestre, C.; Echarri-Iribarren, F. Healthy Climate and Energy Savings: Using Thermal Ceramic Panels and Solar Thermal Panels in Mediterranean Housing Blocks. *Energies* **2018**, *11*, 2707. [CrossRef]

14. Knight, E. Xaar: Innovative inkjet technology for the ceramic tile industry. In *Digital Decoration of Ceramic Tiles*; ACIMAC: Modena, Italy, 2009; pp. 70–73.
15. Hutchings, I. Ink-jet Printing for the Decoration of Ceramic Tiles: Technology and opportunities. In Proceedings of the XI Congreso Mundial de la Calidad del Azulejo y del Pavimento QUALICER 10, Castellón, Spain, 15 February 2010.
16. Echarri, V.; Salvador, M.; Ramírez, G.; Espinosa, A. Lesiones en Paneles Fenólicos de Madera Baquelizada: Diagnóstico e Intervención. In Proceedings of the 4th Congreso de Patología y Rehabilitación de Edificios (PATORREB), Santiago de Compostela, Spain, 15 February 2015; p. 206.
17. CTE. Código Técnico de la Edificación. R/D 314/2006, de 17 de Marzo. Available online: <http://www.codigotecnico.org/images/stories/pdf/realDecreto/RD3142006.pdf> (accessed on 9 September 2017).
18. Mossa, R.W.; Henshall, P.; Arya, F.; Shire, G.S.F.; Hyde, T.; Eames, P.C. Performance and operational effectiveness of evacuated flat plate solar collectors compared with conventional thermal, PVT and PV panels. *Appl. Energy* **2018**, *216*, 588–601. [[CrossRef](#)]
19. Lamnatou, C.; Notton, G.; Chemisana, D.; Cristofari, C. The environmental performance of a building-integrated solar thermal collector, based on multiple approaches and life-cycle impact assessment methodologies. *Build. Environ.* **2015**, *87*, 45–58. [[CrossRef](#)]
20. Kavanaugh, S.P.; Rafferty, K. *Ground-Source Heat Pump: Design of Geothermal Systems for Commercial and Institutional Buildings*; ASHRAE Inc.: Atlanta, GA, USA, 1997.
21. Rosiek, S.; Batlles, F.J. Shallow geothermal energy applied to a solar-assisted air-conditioning system in southern Spain: Two-year experience. *Appl. Energy* **2012**, *100*, 267–276. [[CrossRef](#)]
22. Echarri Iribarren, V.; Espinosa Fernández, A.; Galiano Garrigós, A. Energy efficiency on flooded roofs: The University of Alicante Museum. *WIT Trans. Eng. Sci.* **2016**, *106*, 163–176.
23. Echarri, V.; Espinosa, A.; Rizo, C. Thermal Transmission through Existing Building Enclosures: Destructive Monitoring in Intermediate Layers versus Non-Destructive Monitoring with Sensors on Surfaces. *Sensors* **2017**, *17*, 2848. [[CrossRef](#)]
24. Feijó-Muñoz, J.; Pardal, C.; Echarri, V.; Fernández-Agüera, J.; Assiego de Larriva, R.; Montesdeoca Calderín, M.; Poza-Casado, I.; Padilla-Marcos, M.A.; Meiss, A. Energy impact of the air infiltration in residential buildings in the Mediterranean area of Spain and the Canary islands. *Energy Build.* **2019**, *188–189*, 226–238.
25. UNE-EN ISO 13790: 2011. *Energy Performance of Buildings. Calculation of Energy Use for Space Heating and Cooling*; Spanish Association for Standardization and Certification (AENOR): Madrid, Spain, 2011.
26. Albatici, R.; Tonelli, A.M.; Chiogna, M.A. comprehensive experimental approach for the validation of quantitative infrared thermography in the evaluation of building thermal transmittance. *Appl. Energy* **2015**, *141*, 218–228. [[CrossRef](#)]
27. ISO 9869-1:2014. *Thermal Insulation—Building Elements—In Situ Measurement of Thermal Resistance and Thermal Transmittance—Part 1: Heat Flow Meter Method*; International Organization for Standardization (ISO): Geneva, Switzerland, 2014; Available online: <https://www.iso.org/standard/59697.html> (accessed on 1 November 2017).
28. Soares, N.; Martins, C.; Gonçalves, M.; Santos, P.; Simões da Silva, L.; Costa, J.J. Laboratory and in-situ non-destructive methods to evaluate the thermal transmittance and behavior of walls, windows, and construction elements with innovative materials: A review. *Energy Build.* **2019**, *182*, 88–110. [[CrossRef](#)]
29. Márquez, J.A.; Bohórquez, M.M.; Melgar, S.G. A New Metre for Cheap, Quick, Reliable and Simple Thermal Transmittance (U-Value) Measurements in Buildings. *Sensors* **2017**, *17*, 2017. [[CrossRef](#)]
30. Theodosioua, T.; Tsikaloudakia, K.; Bikasa, D. Analysis of the Thermal Bridging Effect on Ventilated Facades. *Procedia Environ. Sci.* **2017**, *38*, 397–404. [[CrossRef](#)]
31. Ghaffarianhoseini, A.; Zhang, T.; Nwadigo, O.; Naismith, N.; Tookey, J.; Raahemifar, K. Application of nD BIM Integrated Knowledge-based Building Management System (BIM-IKBMS) for inspecting post-construction energy efficiency. *Renew. Sustain. Energy Rev.* **2017**, *72*, 935–949. [[CrossRef](#)]
32. Directive, E. 91/ec of the European parliament and of the council of 16 December 2002 on the energy performance of buildings. *Off. J. Eur. Communities* **2002**, *4*, L1.

33. HULC. Herramienta Unificada Lider-Calener. Orden FOM/1635/2013, de 10 de Septiembre (BOE de 12 de septiembre), por la que se Actualiza el Documento Básico DB HE «Ahorro de Energía», del CTE. Available online: <https://www.codigotecnico.org/index.php/menu-recursos/menu-aplicaciones/282-herramientaunificada-lider-calener.html> (accessed on 9 September 2017).
34. European Commission. Action Plan for Energy Efficiency: Realising the Potential. Commission Staff Working Document. 2006, p. 545. Available online: <http://ec.europa.eu/transparency/regdoc/rep/1/2006/ES/1-2006-545-ES-F1-1.Pdf> (accessed on 16 May 2019).
35. Rahimpoura, Z.; Faccani, A.; Azuatalam, D.; Chapman, A.; Verbič, G. Using Thermal Inertia of Buildings with Phase Change Material for Demand Response. *Energy Procedia* **2017**, *121*, 102–109. [CrossRef]
36. Gaspar, K.; Casals, M.; Gangolells, M. A comparison of standardized calculation methods for in situ measurements of façades U-value. *Energy Build.* **2016**, *130*, 592–599. [CrossRef]
37. Bienvenido-Huertas, D.; Moyano, J.; Marin, D.; Fresco-Contreras, R. Review of in situ methods for assessing the thermal transmittance of walls. *Renew. Sustain. Energy Rev.* **2019**, *102*, 356–371. [CrossRef]
38. Echarri, V. Thermal Ceramic Panels and Passive Systems in Mediterranean Housing: Energy Savings and Environmental Impacts. *Sustainability* **2017**, *9*, 1613. [CrossRef]
39. Choudhury, B.; Saha, B.B.; Chatterjee, P.K.; Sarkar, J.P. An overview of developments in adsorption refrigeration systems towards a sustainable way of cooling. *Appl. Energy* **2013**, *104*, 554–567. [CrossRef]
40. Bataineh, K.; Taamneh, Y. Review and recent improvements of solar sorption cooling systems. *Energy Build.* **2016**, *128*, 22–37. [CrossRef]
41. Sarbu, I.; Sebarchievici, C. Review of solar refrigeration and cooling systems. *Energy Build.* **2013**, *67*, 286–297. [CrossRef]
42. Balghouthi, M.; Chahbani, M.H.; Guisan, A. Investigation of a solar cooling installation in Tunisia. *Appl. Energy* **2012**, *98*, 138–148. [CrossRef]
43. Marrasso, E.; Roselli, C.; Sasso, M.; Tariello, F. Analysis of a Hybrid Solar-Assisted Trigeneration System. *Energies* **2016**, *9*, 705. [CrossRef]
44. Sancho Ávila, J.M.; Riesco Martín, J.; Jiménez Alonso, C.; Sánchez de Cos, M.D.; Montero Cadalso, J.; López Bartolomé, M. Atlas de Radiación Solar en España utilizando datos del SAF de Clima de EUMETSAT. Madrid. 2005. Available online: [http://www.aemet.es/documentos/es/serviciosclimaticos/datosclimatologicos/atlas\\_radiacion\\_solar/atlas\\_de\\_radiacion\\_24042012.pdf](http://www.aemet.es/documentos/es/serviciosclimaticos/datosclimatologicos/atlas_radiacion_solar/atlas_de_radiacion_24042012.pdf) (accessed on 10 March 2019).
45. Aroca-Delgado, R.; Pérez-Alonso, J.; Callejón-Ferre, A.J.; Velázquez-Martí, B. Compatibility between Crops and Solar Panels: An Overview from Shading Systems. *Sustainability* **2018**, *10*, 743. [CrossRef]
46. Valančius, R.; Jurelionis, A.; Jonynas, R.; Katinas, V.; Perednis, E. Analysis of Medium-Scale Solar Thermal Systems and Their Potential in Lithuania. *Energies* **2015**, *8*, 5725–5737. [CrossRef]
47. Prieto, C.; Rodríguez, A.; Patiño, D.; Cabeza, L.F. Thermal energy storage evaluation in direct steam generation solar plants. *Sol. Energy* **2018**, *159*, 501–509. [CrossRef]
48. Corona, B.; de la Rúa, C.; San Miguel, G. Socio-economic and environmental effects of concentrated solar power in Spain: A multiregional input output analysis. *Sol. Energy Mater. Sol. Cells* **2016**, *156*, 112–121. [CrossRef]
49. LCDN Database. Available online: <https://eplca.jrc.ec.europa.eu/LCDN/> (accessed on 9 March 2019).
50. IDAE. Informe de Precios Energéticos Regulados. Julio 2017. Available online: [http://www.idae.es/sites/default/files/estudios\\_informes\\_y\\_estadisticas/tarifas\\_reguladas\\_julio\\_2017.pdf](http://www.idae.es/sites/default/files/estudios_informes_y_estadisticas/tarifas_reguladas_julio_2017.pdf) (accessed on 9 March 2019).

